

Effects of Holothurian Glycosaminoglycan on the Sensitivity of Lung Cancer to Chemotherapy

Integrative Cancer Therapies
Volume 19: 1–10
© The Author(s) 2020
Article reuse guidelines:
sagepub.com/journals-permissions
DOI: 10.1177/1534735420911430
journals.sagepub.com/home/ict


Cunzhi Lin, MD¹, Xinhong Zhu, MD³, Qing Jin, MM⁴, Aihua Sui, MM², Jinfeng Li, MM², and Liyan Shen, MD² 

Abstract

Sea cucumber is a kind of food. Holothurian glycosaminoglycan (hGAG) is extracted from the body wall of the sea cucumber. Administration of hGAG and cisplatin (DDP) together to treat lung cancer was investigated. Lung adenocarcinoma A549 cells were cultured and divided into 4 groups: control group, hGAG 100 µg/mL group, DDP 3 µg/mL group, and hGAG 100 µg/mL + DDP 3 µg/mL group. Cell inhibition and apoptosis was evaluated by CCK8 and Hoechst33258 staining. Cell cycle was tested by Annexin V-FITC/PI (propidium iodide) double-staining and flow cytometry. The expression of mRNA and protein of Bcl-2, Bax, caspase-3, and survivin were detected by reverse transcriptase-polymerase chain reaction and Western blot, respectively. The results showed that hGAG combined with DDP enhanced the inhibitory effect of DDP on A549 lung cells through apoptosis pathway. The mechanism of apoptosis may be related to the reduction of Bcl-2 and survivin, as well as the ascension of Bax and caspase-3. hGAG could promote A549 cell cycle arrest in G1 and G2 phase and improve the DDP chemotherapy effects on A549 cells.

Keywords

holothurian glycosaminoglycan, hGAG, cisplatin, DDP, Bcl-2, Bax, caspase-3, survivin, chemotherapy, lung cancer

Submitted June 13, 2019; revised January 2, 2020; accepted January 31, 2020

Introduction

Sea cucumbers are delicious, nutrient-rich, and of high medicinal values. There are about 1100 species in the world. It has been found that sea cucumber contains many kinds of substances with important biological activities, such as sea cucumber polysaccharides, sea cucumber saponins, peptides, and sea cucumber gangliosides. Thirty years ago, an acidic mucopolysaccharide was extracted from the body wall of edible sea cucumber, which contains galactose, hexuronic acid, fucose, and sulfate. There are 2 main types of polysaccharides in sea cucumber: one is mucopolysaccharide, also called holothurian glycosaminoglycan (hGAG), which is composed of DN-acetylaminogalactose, D-glucuronic acid, and L-fucose; the other is sea cucumber fucoidan, a linear homopolysaccharide composed of L-fucose. Although the glycosyl composition of the 2 types is not the same, the sugar chains of both are rich in sulfate groups (about 32%). This special structure is unique to sea cucumber polysaccharides. Modern pharmacological studies have shown that sea cucumber polysaccharides or hGAG have a variety of pharmacological activities.¹⁻⁵

Worldwide, lung cancer is the leading cause of cancer-related mortality,⁶⁻¹² and it is also one of the most common malignancies.¹³ There are about 1.6 million people dying from lung cancer every year globally,¹⁴ accounting for 19.4% of total cancer mortality, and the 5-year overall survival rate is <20%.¹⁵⁻¹⁸ In China, whether in rural or urban areas, the average mortality rate of lung cancer is higher than that of the remainder of the world, and the total 5-year survival rate is 10% to 15%. The World Health Organization predicted that China would attain the highest lung cancer

¹Department of Pulmonary Medicine, Affiliated Hospital of Qingdao University, Qingdao, Shandong Province, China

²Department of Respiratory & Critical Care Medicine, Affiliated Hospital of Qingdao University, Qingdao, Shandong, China

³Internal Medicine, Qingdao Municipal Hospital, Qingdao, Shandong, China

⁴Department of Intensive Care Unit, The 903rd Hospital of People's Liberation Army, Hangzhou, Zhejiang, China

Corresponding Author:

Liyan Shen, Endocrinology Department, Affiliated Hospital of Qingdao University, 16, Jiangsu Road, Qingdao, Shandong 266555, China.
Email: slycz@126.com



incidence in the world, and that the number of lung cancer deaths among Chinese patients would reach 1 million in 2025.^{18,19} Lung cancer is divided into small cell lung cancer and non-small cell lung cancer (NSCLC) in histopathology; the corresponding proportions are about 15% and 85%, respectively.^{20,21} NSCLC is the most common lung cancer, and more than 50% of NSCLC is adenocarcinoma.

Sea cucumber is a kind of food in Asia. hGAG is an important biologically active compound that can be extracted from the body wall of the sea cucumber.²² hGAG has a number of unique biological properties, including antitumor, anticoagulant, anti-inflammatory, antiviral, anti-fibrosis, immune regulation, and anti-neovascularization.^{23,24} Many studies have confirmed the antitumor activity of hGAG,²⁵⁻³³ but it is unknown whether hGAG could increase the sensitivity of tumors to chemotherapeutic agents or not. In 2018, we did some preliminary research in this area.³⁴ In this study, the mechanism of apoptosis of lung adenocarcinoma A549 cells following administration of hGAG and cisplatin (DDP) was investigated. In addition, the cell cycle effects of hGAG on adenocarcinoma A549 cells related to the sensitivity to DDP chemotherapy were also studied.

Materials and Methods

Isolation and Purification of hGAG

hGAG was extracted from the body wall of the sea cucumber *Aposthopus japonicus*. The body wall of fresh sea cucumber *Aposthopus japonicus* (1 kg) was ground into homogenate and diluted to 1 L. During continuous stirring at 60°C for 1 hour, 56 g of KOH was added. The pH was adjusted to 8.5 with cold HCl. Five grams of diastase was added, and the mixture was maintained at 50°C for 3 hours. The pH of the mixture was adjusted to 7.0 with HCl and the precipitate was removed by centrifugation. A 3-fold 95% (v/v) ethanol was added to precipitate the polysaccharides. The formed precipitate was collected and dissolved in distilled water at a ratio of 1:20 (g/mL). A total of 1.5 M KOAc was added into the supernatant and kept at 4°C overnight. Crude hGAG was collected by centrifugation, dissolved in distilled water, dialyzed against distilled water for 36 hours, and lyophilized. The crude hGAG was fractionated by a Q Sepharose Fast Flow column (300 mm × 30 mm) coupled with a peristaltic pump, eluted with a stepwise gradient of 0, 0.75, and 1.5 mol/L NaCl, and detected by phenol-sulfuric acid method. The fractions eluted by 1.5 M aqueous NaCl were pooled, dialyzed, and further purified on a Sephadex 25 column (100 cm × 2.6 cm) with deionized water. The major polysaccharide fractions were pooled and lyophilized. Molecular weight of hGAG was 98.07 kDa. hGAG was endowed by the Key Laboratory of Marine Drugs of Ministry of Education, and Key Laboratory of Glycoscience and Glycotechnology of School of Medicine and Pharmacy, Ocean University of China (Patent Number: 120406).

Cell Culture

The human lung adenocarcinoma cell line A549 was purchased from the American Type Culture Collection (ATCC, Manassas, VA). The cells were cultured in RPMI-1640 (Gibco, Carlsbad, CA) medium, which was supplemented with 10% heat-inactivated fetal bovine serum and 1% pen-strep (100 U/mL penicillin and 100 U/mL streptomycin; Gibco) in a 37°C humidified incubator containing 5% CO₂. All experiments were performed using cells grown to 70% to 80% confluence.

CCK8 Detection

Cell viability was assessed by CCK8 (Beyotime Institute of Biotechnology, Shanghai, China). A549 cells were seeded in 96-well plates at a density of 1×10^4 cells/well and treated with various concentrations of treatment at 37°C for 24, 48, and 72 hours, respectively. Cells were divided into 4 groups: control group, hGAG 100 µg/mL group, DDP 3 µg/mL group (Jiangsu Hansoh Pharmaceutical Group Co, Ltd, Jiangsu, China), and hGAG 100 µg/mL + DDP 3 µg/mL group. Each group included 3 wells, which were washed with 100 µL phosphate-buffered saline (PBS; Hyclone) and contained 10 µL CCK8 + 90 µL complete medium at 37°C for experimental culture, separately. A microplate reader was used to read the optical density (OD) at 450 nm after 15 minutes, 30 minutes, 1 hour, 2 hours, 3 hours, and 4 hours. The inhibition ratio was calculated with the following formula: Growth inhibition ratio (%) = (Absorbance of control group – Absorbance of experimental group)/(Absorbance of control group – Absorbance of blank control group) × 100%.

The synergistically inhibitory effect of drug combinations was analyzed by the coefficient of drug interaction (CDI). CDI is calculated as follows: $CDI = AB/(A \times B)$. According to the absorbance of each group, AB is the ratio of the combination group to the control group, and A or B is the ratio of the single agent group to the control group. Accordingly, if the CDI value is ≥ 1 , or < 1 , it indicates that the drugs are antagonistic additive or synergistic, respectively. A CDI of < 0.7 indicates that the drugs are significantly synergistic.²⁹

Hoechst 33258 Staining

A549 cells grown on a sterile cover slips in 6-well plates were treated with various concentrations of agents for 48 hours. The culture medium containing compound was removed, and the cells were fixed in fixative (Beyotime) for 15 minutes. After washing twice using PBS, the cells were stained with 0.5 mL of Hoechst 33258 (Beyotime) for 5 minutes and washed again twice using PBS. A drop of prolonged gold anti-fade reagent (Beyotime) was added, and the cells were observed using fluorescence microscopy (Olympus Co, Japan) under 350 nm excitation and 460 nm emission.

Table 1. Primer Sequences for Reverse Transcriptase-Polymerase Chain Reaction.

Genes	Forward	Reverse
<i>Bax</i>	5'-AGCGACTGATGTCCCTGTCT-3'	5'-CTCAGCCCATCTTCTTCCAG-3'
<i>Bcl-2</i>	5'-ATGTGTGTGGAGAGCGTCAA-3'	5'-ACCTACCCAGCCTCCGTTAT-3'
<i>Survivin</i>	5'-GCCCAGTGTTTCTTCTGCTT-3'	5'-TCTCCGCAGTTTCTCAAAT-3'
<i>Caspase-3</i>	5'-GTGGAGGCCGACTTCTTGTGA-3'	5'-TGTCGGCATACTGTTTCAGC-3'
<i>GAPDH</i>	5'-GCACCGTCAAGGCTGAGAAC-3'	5'-TGGTGAAGACGCCAGTGGA-3'

RNA Isolation and Quantitative Real-Time Polymerase Chain Reaction

A549 cells were seeded in 6-well plates, and when the cells reached 70% to 80% confluence, they were treated with various concentrations of agents for 48 hours, at 37°C. Total RNA was extracted from A549 cells using TRIzol (Invitrogen, Carlsbad, CA) according to the manufacturer's instructions, measured by a microplate reader. Single-stranded cDNA was prepared by reverse transcriptase with oligo-dT primer according to the manufacturer's instructions (TaKaRa Biomedical Technology Co, Ltd, Dalian, China). cDNA was used for polymerase chain reaction (PCR) amplification, and the gene expression was performed by reverse transcriptase-PCR (RT-PCR), measured using the SYBR Green PCR master mix (TaKaRa). Primers (Sangon Biotech Co, Ltd, Shanghai, China) for *Bax*, *Bcl-2*, *survivin*, *caspase-3*, and *GAPDH* gene were designed (Table 1). Real-time PCR was followed by melting curve analysis with the following cycling program: initial denaturation at 95°C for 10 minutes, followed by 40 cycles of denaturation at 95°C for 5 seconds, annealing at 60°C for 30 seconds, and extension at 60°C for 3 minutes. Fold change in mRNA expression was calculated by the $2^{-\Delta\Delta^{ct}}$ method.

Western Blot Analysis

A549 cells were seeded in 6-well plates, cultured for 12 hours, and then incubated at 37°C with reagents of various concentrations for 48 hours. Protein was extracted from A549 cells in mixtures of RIPA, PIC, and PMSF (RIPA:PIC:PMSF = 100:2:1, Beyotime) with an ultrasonicator on ice, and then nuclei and cell debris were removed by centrifugation at 13 000 relative centrifugal force for 15 minutes, at 4°C. Total protein concentration was determined using BCA Kit (Beyotime). Protein was separated by SDS-PAGE (Beyotime), and then electro-transferred onto a nitrocellulose membrane (Millipore, MA). Nitrocellulose blots were incubated in PBST buffer (Beijing Solarbio Science and Technology Co, Ltd, China), blocked with 5% skim milk powder for 1 hour at room temperature, and the membrane was incubated with primary antibodies overnight at 4°C. After washing 3 times with PBST buffer for 15 minutes, the nitrocellulose membranes were incubated with goat anti-rabbit immunoglobulin G second antibody for 1

hour. After washing 3 times again with PBST buffer for 15 minutes, the results of immune-complex bands were observed using chemiluminescence photographs with enhanced chemiluminescence (ECL, Pierce Chemical, Rockford, IL). Antibodies used in this study were Rabbit anti-human survivin, *Bax*, *Bcl-2*, *caspase-3* and anti- β -Tubulin antibody, and goat anti-rabbit immunoglobulin G second antibody (Abcam, Cambridge, MA, diluted 1:1000).

Flow Cytometric Analyses of Apoptosis and Cell Cycle

Apoptotic cells were determined by Annexin V-FITC/PI Apoptosis Kit (BD Biosciences, San Jose, CA) according to the manufacturer's instructions. Cells were treated with various concentrations of agents for 48 hours as for the Western blot. Then the cells were washed with PBS and harvested with trypsin/EDTA (ethylenediaminetetraacetic acid; Hyclone). The cells were centrifuged for 5 minutes and then washed twice with PBS, stained with FITC and propidium iodide (PI) for 15 minutes at room temperature. After incubation, fluorescence of cells was read by a flow cytometer (BD Biosciences, Franklin Lakes, NJ) immediately. For the cell cycle analysis, cells were harvested as apoptotic, and immediately fixed with 70% ethanol, then stained with PI staining buffer (Beyotime) at 37°C in the dark for 30 minutes. After incubation, cells were analyzed by a FACS Calibur Flow Cytometer.

Statistical Analysis

All experiments were repeated at least 3 times. The data were evaluated using 1-way analysis of variance for unpaired data using SPSS statistical software for Windows, version 22.0 (SPSS Inc, IBM, Chicago, IL), with error bars representing the mean \pm SD. A value of $P < .05$ was considered statistically significant.

Results

The Inhibition Effects of hGAG and DDP on A549 Cells Line

To investigate the effects of hGAG and DDP on A549 cells viability, the CCK-8 assay was performed. We measured the OD value and proliferative activity of A549 cells with

Table 2. The OD Value and Growth Inhibition on A549 Cell in Different Concentrations and Time-Points (Mean \pm SD, n = 3).

Groups	24 Hours		48 Hours		72 Hours	
	OD	IR (%)	OD	IR (%)	OD	IR (%)
Control*	1.800 \pm 0.068	0	3.076 \pm 0.048	0	3.686 \pm 0.045	0
hGAG*	1.495 \pm 0.019	16.85 \pm 3.57	2.062 \pm 0.027	32.94 \pm 1.71	2.340 \pm 0.075	36.53 \pm 1.33
DDP*	1.398 \pm 0.015	22.21 \pm 3.70	1.696 \pm 0.034	44.88 \pm 1.37	1.964 \pm 0.040	46.73 \pm 5.42
DDP + hGAG**	1.018 \pm 0.086	43.30 \pm 6.26	0.670 \pm 0.056	78.18 \pm 2.17	0.800 \pm 0.019	78.30 \pm 4.60

Abbreviations: OD, optical density; IR, inhibition ratio; hGAG, holothurian glycosaminoglycan; DDP, administration of hGAG and cisplatin.

* $P < .05$ compared with the control group.

** $P < .05$ hGAG + DDP group compared with DDP group. The IR was most obviously in DDP + hGAG group. $P < .05$ was considered statistically significant.

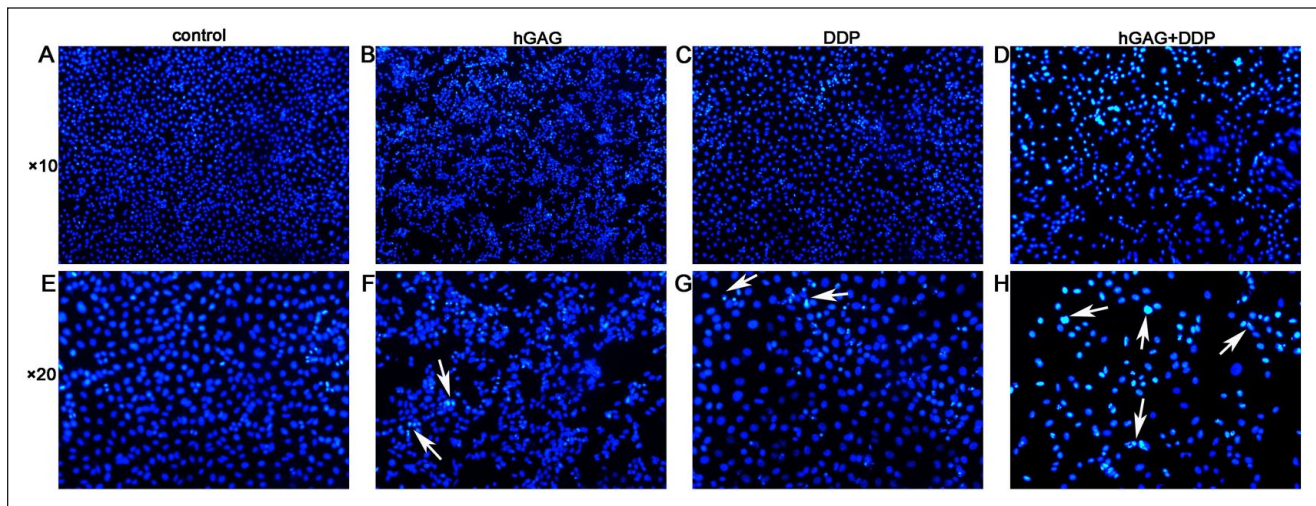


Figure 1. A549 cells were treated with various concentrations of samples for 48 hours. The cells stained by Hoechst33258 and images were captured using a fluorescence microscope. White arrow showed the apoptotic, shrunken, hyperchromatic, and pyknotic apoptotic cells.

various concentrations for different periods of time (Table 2 shows data at 1 hour after CCK-8 was performed). It was observed that hGAG and DDP exhibited concentration and time-dependent inhibitory effects on the proliferation of A549 cells ($P < .05$). The inhibitory effect was most clear in hGAG + DDP group ($P < .05$). CDI was 0.94, 0.75, and 0.78 at 24 hours, 48 hours, and 72 hours, respectively.

The Apoptosis Effects of hGAG and DDP on A549 Cells

We detected the apoptotic A549 cells by Hoechst33258 staining. There were no obvious apoptotic cells in control group, while we observed shrunken, hyperchromatic, and pyknotic cells in hGAG, DDP, and hGAG + DDP groups. Compared with other groups, the cell numbers were the lowest and the apoptotic cells were the most obvious in the hGAG + DDP group (Figure 1). The apoptosis rates of A549 cells were $3.68 \pm 1.10\%$, $22.27 \pm 2.42\%$, $24.19 \pm$

4.63% , and $46.97 \pm 3.51\%$ in the control, hGAG, DDP, and hGAG + DDP groups, respectively. Apoptosis was significantly increased compared with the control group ($F = 92.45$, $P < .05$). The study also evaluated the ratio of apoptosis in the DDP + hGAG group compared with the DDP group. The results from flow cytometry revealed that DDP and hGAG induced A549 cells apoptosis. hGAG increased the ratio of apoptosis induced by DDP ($P < .05$; Figure 2).

The mRNA Expression of Bax, Caspase-3, Bcl-2, and Survivin in Different Groups

We detected the mRNA expression of Bax, caspase-3, Bcl-2, and survivin in different groups by RT-PCR. Our results indicated that gene expression of Bax and caspase-3 were upregulated in hGAG, DDP, and hGAG + DDP groups compared with the control group ($P < .05$). In contrast, Bcl-2 and survivin were downregulated in the 3 groups ($P < .05$). The significant differences were in all groups

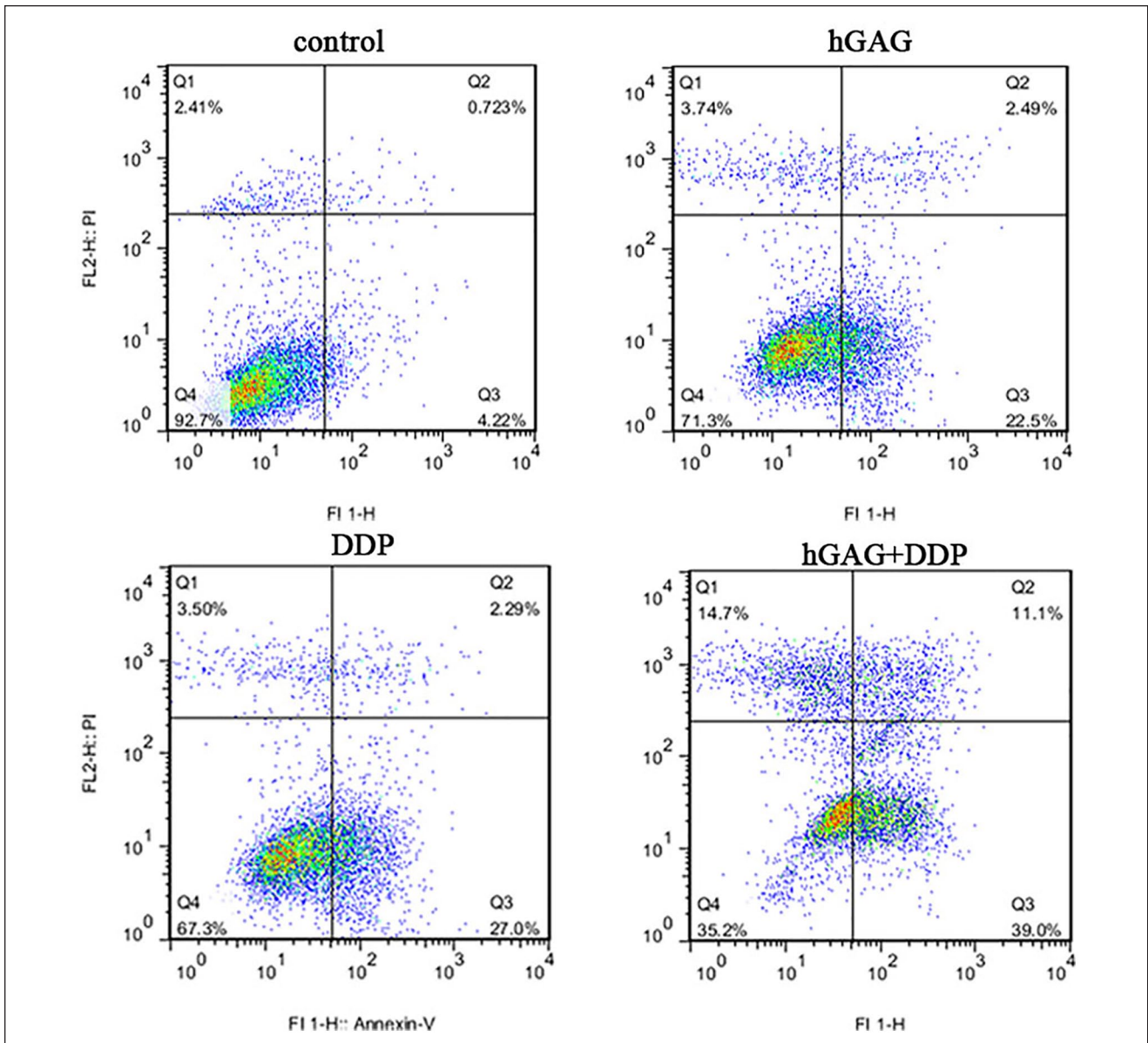


Figure 2. A549 cells were treated with various concentrations of samples for 48 hours. Cell apoptosis tested by Annexin V-FITC/PI flow cytometry; proportion of apoptotic cells was measured.

($P < .05$), with the most pronounced effect in the hGAG + DDP group ($P < .05$; Figure 3).

The Protein Expression of Bcl-2, Bax, Survivin, and Caspase-3 in Different Groups

The protein expression of Bcl-2, Bax, survivin, and caspase-3 was detected by Western blot analysis (Figure 4A). A549 cells were conditioned in the presence of DDP and hGAG. The protein expression of Bcl-2 and survivin was significantly downregulated, while Bax and caspase-3 were significantly increased compared with the control group (P

$< .05$). Compared with the DDP group, the protein expression was obviously different in the DDP + hGAG group ($P < .05$; Figure 4B).

The Effect of hGAG and DDP on Cell Cycle Distribution

As compared with the control group (G1: $60.500 \pm 1.153\%$), treatment with hGAG (100 $\mu\text{g/mL}$), showed a blocking of A549 cells in the G1 phase ($69.430 \pm 0.762\%$; Table 3). Treatment with 3 $\mu\text{g/mL}$ DDP showed arrest of cells in S phases compared with S phase cells ($17.450 \pm$

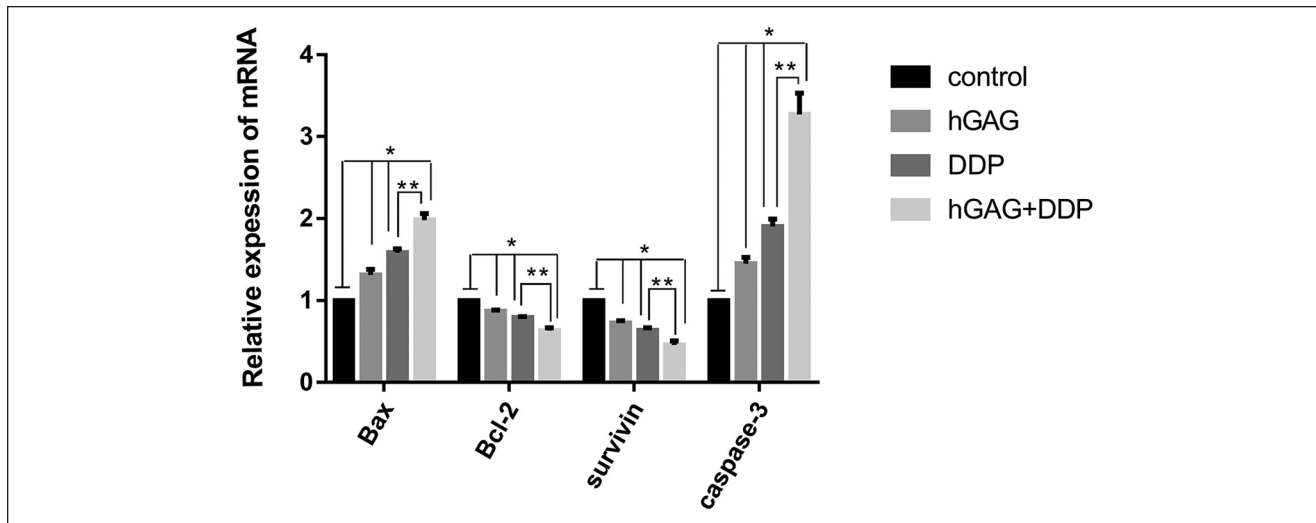


Figure 3. A549 cells were treated with various concentrations of samples for 36 hours. The mRNA expression of Bcl-2, Bax, survivin, and caspase-3 in different groups. * $P < .05$ compared with the control group; ** $P < .05$ hGAG + DDP group compared with DDP group.

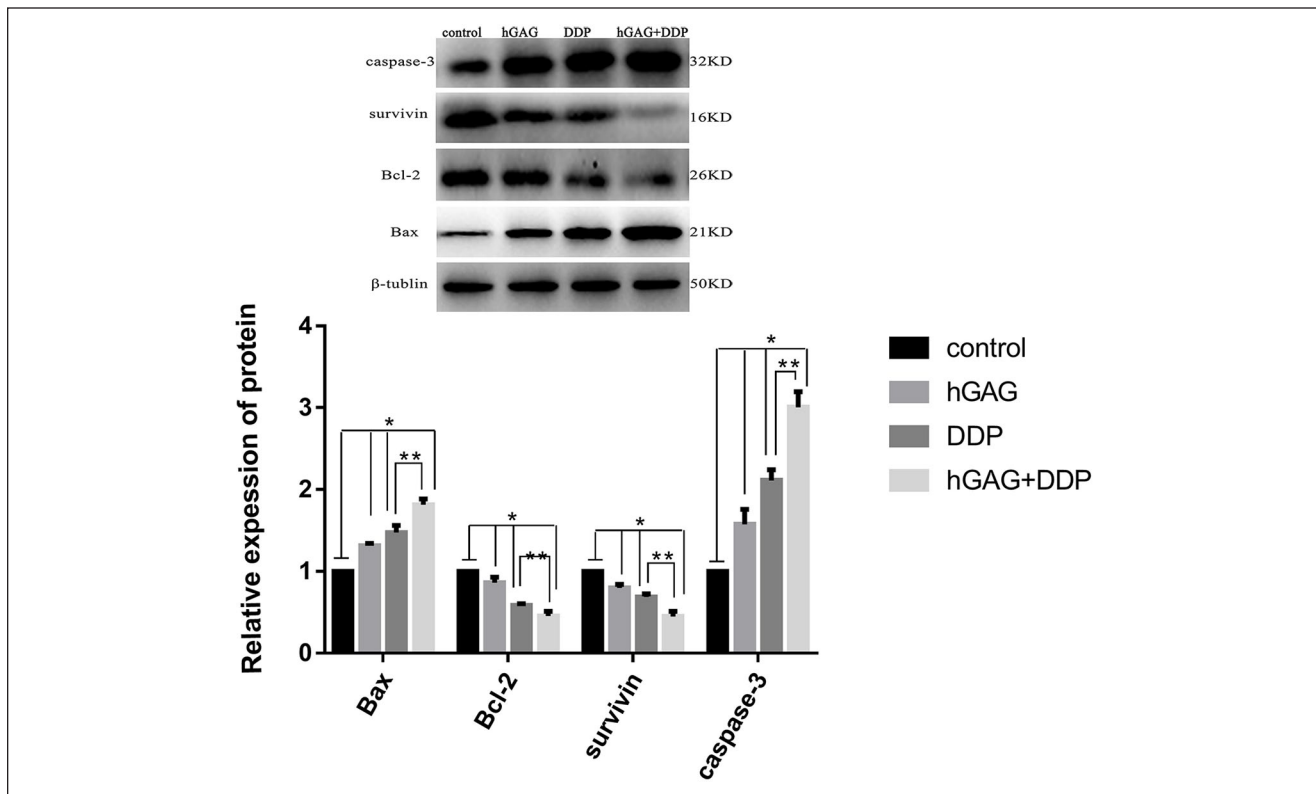


Figure 4. A549 cells were treated with various concentrations of samples for 48 hours. The protein expression of Bcl-2, Bax, survivin, and caspase-3 in A549 cells detected by Western blotting in different groups. * $P < .05$ compared with the control group; ** $P < .05$ hGAG + DDP group compared with DDP group.

0.837%) in the control group (Figure 5). Combination treatment of 3 $\mu\text{g/mL}$ DDP and hGAG (100 $\mu\text{g/mL}$) simultaneously showed an increase in the percentages of cells in G1 phase cells ($56.803 \pm 0.798\%$) and G2 phase cells (12.270

$\pm 0.420\%$) compared with the DDP group (G1: $43.887 \pm 2.365\%$, G2: $4.043 \pm 0.196\%$). Altogether, the hGAG could promote cell cycle arrest in G1 and G2 phases to chemotherapy of DDP in A549 cells.

Table 3. The Cell Cycle Arrested on Lung Adenocarcinoma A549 Cells in Different Concentrations for 48 Hours (Mean \pm SD, n = 3).

Groups	G1 (%)	S (%)	G2 (%)
Control	60.500 \pm 1.153	17.450 \pm 0.837	17.993 \pm 0.871
hGAG*	69.430 \pm 0.7621	9.750 \pm 0.66	6.127 \pm 0.277
DDP*	43.887 \pm 2.365	47.740 \pm 2.227	4.043 \pm 0.196
DDP + hGAG**	56.803 \pm 0.798	27.697 \pm 0.699	12.270 \pm 0.420

Abbreviations: hGAG, holothurian glycosaminoglycan; DDP, administration of hGAG and cisplatin.

*P < .05 compared with the control group (hGAG: G1, DDP: S).

**P < .05 hGAG + DDP group compared with DDP group (G1, G2). P < .05 was considered statistically significant.

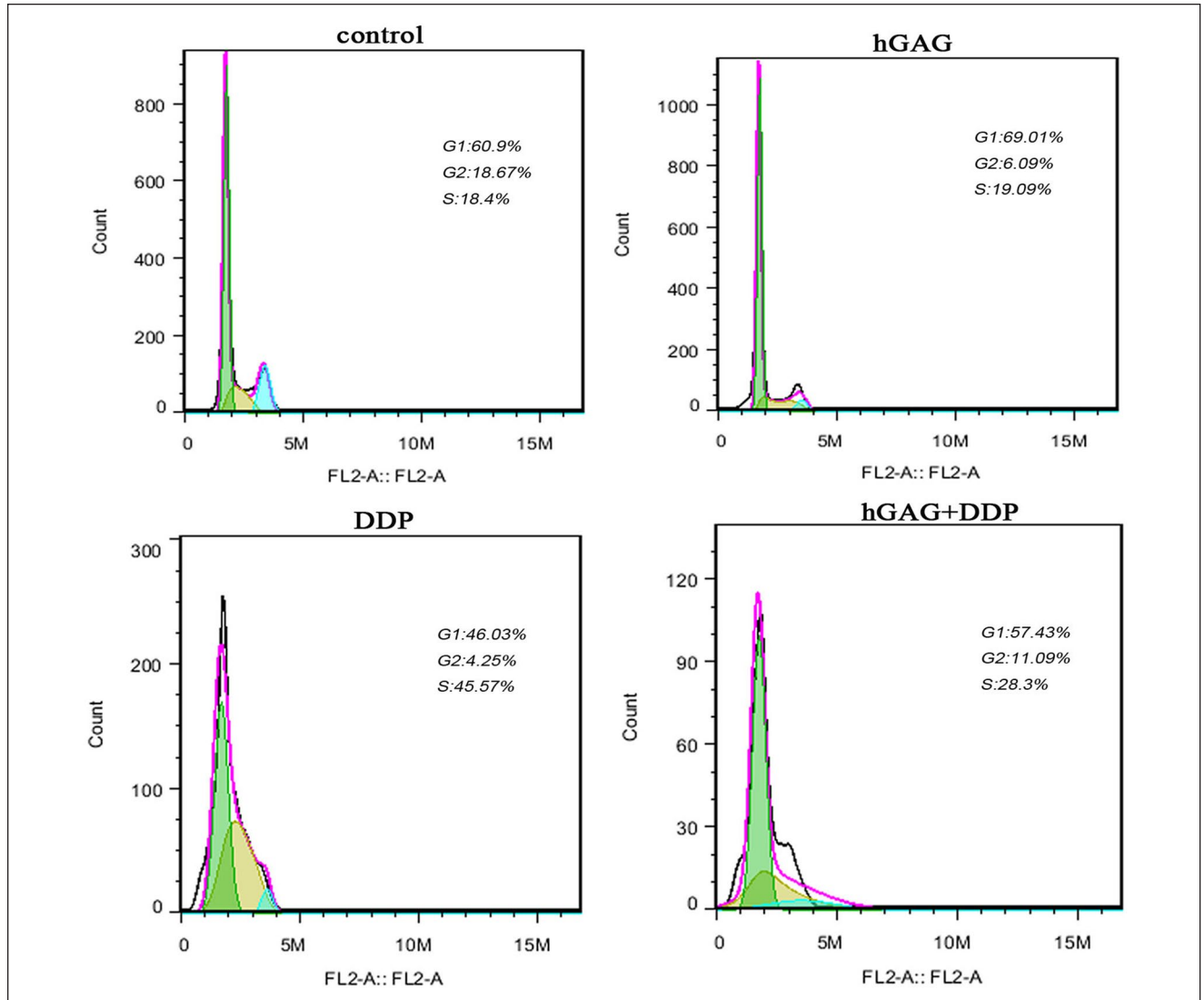


Figure 5. A549 cells were treated with various concentrations of samples for 48 hours. Cell cycle changes and the distribution of each cell cycle phase in A549 cells analyzed by flow cytometry assays.

Discussion

HGAG is a holothurian glycosaminoglycan extracted from the body wall of sea cucumber. The antitumor effect of hGAG has been studied quite widely in recent years, as well as the mechanism of hGAG for the modulation of immunoreactivities,^{6,25} antiangiogenesis,³ induction of apoptosis, and cell cycle inhibition.²⁶⁻²⁸ Apoptosis and cell cycle inhibition are the most studied mechanisms. Both Bcl-2 and Bax belong to the Bcl-2 family; their oncogene activity will be enhanced when Bcl-2 is strongly expressed or Bax expressed at low levels. So the ratio of Bax/Bcl-2 may regulate the initiation of the apoptotic signal.^{35,36} In current research on tumor cell division and inhibition of apoptosis, survivin is the strongest inhibitor of apoptosis, belonging to the apoptosis inhibition family.³⁶⁻³⁹ Caspase-3 is an important apoptosis regulator and key enzyme in the cysteinyl aspartate-specific proteinase (caspase) family. Most factors initiate apoptosis through the caspase-3-mediated pathway.^{37,38,40}

Activated caspase-3 is an important signaling molecule in the apoptosis pathway and is associated with the activation of caspase-9.⁴⁰ The antiapoptotic effect of survivin is connected with caspase-3 activation.⁴¹ Survivin can directly inhibit the activity of caspase-3 downstream of the apoptotic pathway and indirectly inhibit the activation of caspase-3 by means of caspase-9. The homodimers of Bax could be increased on account of Bax strongly expressing; furthermore, Bax overexpression could alter mitochondrial transmembrane potential, activate caspase-7 and caspase-3 downstream, accomplish substrate excision, and accelerate apoptosis by combining with mitochondrial membrane, as well as initiating a cascade of caspase.⁴² In contrast, when the homodimer of Bax decreases, the heterodimer of Bax/Bcl-2 might increase, and apoptosis will be inhibited when Bcl-2 is strongly expressed.⁴²

Caspase-3 is the main performer of the apoptotic procedure, activating DNA fragments, leading to DNA degradation, resulting in nuclear fragmentation, and inducing apoptosis by cascade reactions.⁴³ As is noted above, both survivin and Bcl-2 can inhibit apoptosis through inhibiting caspase-3. Bcl-2 can inhibit mitochondrial releasing cytochrome C by acting on caspase-3 upstream, whereas survivin can inhibit caspase-3 downstream of the apoptotic pathway.⁴³ Our results indicate that both Bcl-2 and survivin mRNA and protein expression might be decreased when A549 cells were conditioned in the absence or presence of either DDP or hGAG; however, the expression of Bax and caspase-3 mRNA and protein could be increased at the same time. The expression of mRNA and protein was most pronounced in both the DDP group and the hGAG group. The results of Western blotting coincided with RT-PCR result; nevertheless, there is a significant difference between the groups in mRNA and protein expression. Low expression of Bcl-2 and survivin mRNA and protein could

upregulate caspase-3, thereby the activity and function of caspase-3 could be increased, while the apoptosis of A549 cells was promoted. On the other hand, Bax overexpression can initiate the caspase cascade by activating caspase-3 downstream, which may promote apoptosis in A549 cells.

Aberrant regulation of cell cycle is closely related to cancer progression and development. The cell cycle can be divided into inter-phase and cell division, including G0, G1, S, G2, and M phases. G1 phase is the main "restriction site."⁴³⁻⁴⁵ Whether cells proliferate or not is determined by whether the cells could go through the G1 phase to the S phase.^{45,46} DDP is a nonspecific cell cycle phase agent and could suppress DNA replication by forming DDP-DNA cross-linking with DNA.⁴⁷ In this study, DDP could arrest cell proliferation at the S phase, whereas hGAG may arrest cell proliferation at the G1 phase, DDP + hGAG could reduce the S phase arrest while increasing the G1 phase arrest when compared with DDP. Cell proliferation would be inhibited when the G1 phase arrest increases and more cells cannot enter into the S phase.

In conclusion, hGAG, whether in combination with DDP or not, could promote apoptosis and inhibit proliferation of A549 cells; at the same time, hGAG could increase the sensitivity to DDP chemotherapy of A549 cells. The mechanism of hGAG-sensitizing may be associated with low expression of Bcl-2 and survivin mRNA and protein, as well as overexpression of Bax and caspase-3 mRNA and protein. In addition, we consider that the hGAG could promote cell cycle arrest in G1 and G2 phases and raise the chemotherapeutic effects of DDP on A549 cells.

Declaration of Conflicting Interests

The author(s) declared no potential conflicts of interest with respect to the research, authorship, and/or publication of this article.

Funding

The author(s) disclosed receipt of the following financial support for the research, authorship, and/or publication of this article: This project was supported by the Key Laboratory of Marine Drug, Ministry of Education (KLMDUUC201307).

ORCID iD

Liyang Shen  <https://orcid.org/0000-0002-7562-8770>

References

1. Li T, Wang X, Lin C, Zhu X. Research and progression on anti-lung neoplasm activity and the regulation of T cellular immune function by polysaccharide from sea cucumber [in Chinese]. *Chin J Clinicians*. 2014;8:1945-1948.
2. Borsig L, Wang L, Cavalcante MC, et al. Selectin blocking activity of a fucosylated chondroitin sulfate glycosaminoglycan from sea cucumber. Effect on tumor metastasis and neutrophil recruitment. *J Biol Chem*. 2007;282:14984-14991.

3. Zhang W, Lu Y, Xu B, et al. Acidic mucopolysaccharide from *Holothuria leucospilota* has antitumor effect by inhibiting angiogenesis and tumor cell invasion in vivo and in vitro. *Cancer Biol Ther.* 2009;8:1489-1499.
4. Althunibat OY, Ridzwan BH, Taher M, et al. Antioxidant and cytotoxic properties of two sea cucumbers, *Holothuria edulis* lesson and *Stichopus horrens* Selenka. *Acta Biol Hung.* 2013;64:10-20.
5. Morla S. Glycosaminoglycans and glycosaminoglycan mimetics in cancer and inflammation. *Int J Mol Sci.* 2019;20:E1963.
6. Yu L, Xue C, Chang Y, et al. Structure elucidation of fucoidan composed of a novel tetrafucose repeating unit from sea cucumber *Thelenota ananas*. *Food Chem.* 2014;146:113-119.
7. Ustyuzhanina NE, Fomitskaya PA, Gerbst AG, Dmitrenok AS, Nifantiev NE. Synthesis of the oligosaccharides related to branching sites of fucosylated chondroitin sulfates from sea cucumbers. *Mar Drugs.* 2015;13:770-787.
8. Deneka AY, Haber L, Kopp MC, Gaponova AV, Nikonova AS, Golemis EA. Tumor-targeted SN38 inhibits growth of early stage non-small cell lung cancer (NSCLC) in a KRas/p53 transgenic mouse model. *PLoS One.* 2017;12:e0176747.
9. Scrima M, Zito Marino F, Oliveira DM, et al. Aberrant signaling through the HER2-ERK1/2 pathway is predictive of reduced disease-free and overall survival in early stage non-small cell lung cancer (NSCLC) patients. *J Cancer.* 2017;8:227-239.
10. Kolokotroni E, Dionysiou D, Veith C, et al. In silico oncology: quantification of the in vivo antitumor efficacy of cisplatin-based doublet therapy in non-small cell lung cancer (NSCLC) through a multiscale mechanistic model. *PLoS Comput Biol.* 2016;12:e1005093.
11. Kudinov AE, Deneka A. Musashi-2 (MSI2) supports TGF- β signaling and inhibits claudins to promote non-small cell lung cancer (NSCLC) metastasis. *Proc Natl Acad Sci U S A.* 2016;113:6955-6960.
12. Vazquez S, Casal J, Afonso FJA, et al. EGFR testing and clinical management of advanced NSCLC: a Galician Lung Cancer Group study (GGCP 048-10). *Cancer Manag Res.* 2016;8:11-20.
13. Whang YM, Park SI, Trenary IA, et al. LKB1 deficiency enhances sensitivity to energetic stress induced by erlotinib treatment in non-small-cell lung cancer (NSCLC) cells. *Oncogene.* 2016;35:856-866.
14. Rudisch A, Dewhurst MR, Horga LG, et al. High EMT signature score of invasive non-small cell lung cancer (NSCLC) cells correlates with NF κ B driven colony-stimulating factor 2 (CSF2/GM-CSF) secretion by neighboring stromal fibroblasts. *PLoS One.* 2015;10:e0124283.
15. Mizugaki H, Yamamoto N, Nokihara H, et al. A phase I study evaluating the pharmacokinetics and preliminary efficacy of veliparib (ABT-888) in combination with carboplatin/paclitaxel in Japanese subjects with non-small cell lung cancer (NSCLC). *Cancer Chemother Pharmacol.* 2015;76:1063-1072.
16. Castanon E, Rolfo C, Vinal D, et al. Impact of epidermal growth factor receptor (EGFR) activating mutations and their targeted treatment in the prognosis of stage IV non-small cell lung cancer (NSCLC) patients harboring liver metastasis. *J Transl Med.* 2015;13:257.
17. Gridelli C, Camerini A, Pappagallo G, et al. Clinical and radiological features driving patient selection for antiangiogenic therapy in non-small cell lung cancer (NSCLC). *Cancer Imaging.* 2016;16:44.
18. Barnfield PC, Ellis PM. Second-line treatment of non-small cell lung cancer: new developments for tumours not harbouring targetable oncogenic driver mutations. *Drugs.* 2016;76:1321-1336.
19. Hong QY, Wu GM, Qian GS, et al. Prevention and management of lung cancer in China. *Cancer.* 2015;121(suppl 17):3080-3088.
20. Zhang X, Liu S, Liu Y, et al. Economic burden for lung cancer survivors in urban China. *Int J Environ Res Public Health.* 2017;14:E308.
21. Fang JY, Dong HL, Wu KS, Du PL, Xu ZX, Lin K. Characteristics and prediction of lung cancer mortality in China from 1991 to 2013. *Asian Pac J Cancer Prev.* 2015;16:5829-5834.
22. Lee SO, Yang X, Duan S, et al. IL-6 promotes growth and epithelial-mesenchymal transition of CD133+ cells of non-small cell lung cancer. *Oncotarget.* 2016;7:6626-6638.
23. Jung JH, Kim MJ, Lee H, et al. Farnesiferol c induces apoptosis via regulation of L11 and c-Myc with combinational potential with anticancer drugs in non-small-cell lung cancers. *Sci Rep.* 2016;6:26844.
24. Yue Z, Wang A, Zhu Z, et al. Holothurian glycosaminoglycan inhibits metastasis via inhibition of P-selectin in B16F10 melanoma cells. *Mol Cell Biochem.* 2015;410:143-154.
25. Song Y, Jin SJ, Cui LH, Ji XJ, Yang FG. Immunomodulatory effect of *Stichopus japonicus* acid mucopolysaccharide on experimental hepatocellular carcinoma in rats. *Molecules.* 2013;18:7179-7193.
26. Cui C, Cui N, Wang P, Song S, Liang H, Ji A. Sulfated polysaccharide isolated from the sea cucumber *Stichopus japonicus* against PC12 hypoxia/reoxygenation injury by inhibition of the MAPK signaling pathway. *Cell Mol Neurobiol.* 2015;35:1081-1092.
27. You L, Gao Q, Feng M, et al. Structural characterisation of polysaccharides from *Tricholoma matsutake* and their antioxidant and antitumour activities. *Food Chem.* 2013;138:2242-2249.
28. Lu Y, Zhang BY, Dong Q, Wang BL, Sun XB. The effects of *Stichopus japonicus* acid mucopolysaccharide on the apoptosis of the human hepatocellular carcinoma cell line HepG2. *Am J Med Sci.* 2010;339:141-144.
29. Wang D, Wang Z, Tian B, Li X, Li S, Tian Y. Two hour exposure to sodium butyrate sensitizes bladder cancer to anti-cancer drugs. *Int J Urol.* 2008;15:435-441.
30. Lamichhane SP, Arya N, Ojha N, Kohler E, Shastri VP. Glycosaminoglycan-functionalized poly-lactide-co-glycolide nanoparticles: synthesis, characterization, cytocompatibility, and cellular uptake. *Int J Nanomedicine.* 2015;10:775-789.
31. Qian W, Tao L, Wang Y, et al. Downregulation of integrins in cancer cells and anti-platelet properties are involved in holothurian glycosaminoglycan-mediated disruption of the interaction of cancer cells and platelets in hematogenous metastasis. *J Vasc Res.* 2015;52:197-209.
32. Liu X, Liu Y, Hao J, et al. In vivo anti-cancer mechanism of low-molecular-weight fucosylated chondroitin sulfate

- (LFCS) from sea cucumber *Cucumaria frondosa*. *Molecules*. 2016;21:E625.
33. Zhao Y, Zhang D, Wang S, et al. Holothurian glycosaminoglycan inhibits metastasis and thrombosis via targeting of nuclear factor- κ B/tissue factor/Factor Xa pathway in melanoma B16F10 cells. *PLoS One*. 2013;8:e56557.
 34. Jin Q, Zhu XH, Lin CZ, et al. The roles of holothurian glycosaminoglycan combined with cisplatin on proliferation and chemotherapeutic response in A549 human lung adenocarcinoma cell [in Chinese]. *Zhonghua zhong liu za zhi*. 2018;40:252-257.
 35. Bai X, Meng H, Ma L, Guo A. Inhibitory effects of evodiamine on human osteosarcoma cell proliferation and apoptosis. *Oncol Lett*. 2015;9:801-805.
 36. Zhong F, Yang J, Tong ZT, et al. Guggulsterone inhibits human cholangiocarcinoma Sk-ChA-1 and Mz-ChA-1 cell growth by inducing caspase-dependent apoptosis and down-regulation of survivin and Bcl-2 expression. *Oncol Lett*. 2015;10:1416-1422.
 37. Feng W, Fu Y, Zhang Y, et al. Establishment of stable multiple myeloma cell line with overexpressed PDCD5 and its proapoptosis mechanism. *Int J Clin Exp Pathol*. 2015;8:10635-10643.
 38. Wang Y, Kong D, Wang X, Dong X, Tao Y, Gong H. Molecular mechanisms of luteolin induced growth inhibition and apoptosis of human osteosarcoma cells. *Iran J Pharm Res*. 2015;14:531-538.
 39. Jafari N, Zargar SJ, Yassa N, Delnavazi MR. Induction of apoptosis and cell cycle arrest by dorema glabrum root extracts in a gastric adenocarcinoma (AGS) cell line. *Asian Pac J Cancer Prev*. 2016;17:5189-5193.
 40. Guo X, Zhang X, Wang T, Xian S, Lu Y. 3-Bromopyruvate and sodium citrate induce apoptosis in human gastric cancer cell line MGC-803 by inhibiting glycolysis and promoting mitochondria-regulated apoptosis pathway. *Biochem Biophys Res Commun*. 2016;475:37-43.
 41. Shishido SN, Faulkner EB, Beck A, Nguyen TA. The effect of antineoplastic drugs in a male spontaneous mammary tumor model. *PLoS One*. 2013;8:e64866.
 42. Hahnvajjanawong C, Wattanawongdon W, Chomvarin C, et al. Synergistic effects of isomorellin and forbesione with doxorubicin on apoptosis induction in human cholangiocarcinoma cell lines. *Cancer Cell Int*. 2014;14:68.
 43. Elkady AI, Hussein RA, El-Assouli SM. Harmal extract induces apoptosis of hct116 human colon cancer cells, mediated by inhibition of nuclear factor- κ B and activator protein-1 signaling pathways and induction of cytoprotective genes. *Asian Pac J Cancer Prev*. 2016;17:1947-1959.
 44. Nussinov R, Tsai CJ, Muratcioglu S, Jang H, Gursoy A, Keskin O. Principles of K-Ras effector organization and the role of oncogenic K-Ras in cancer initiation through G1 cell cycle deregulation. *Expert Rev Proteomics*. 2015;12:669-682.
 45. Bertoli C, Skotheim JM, de Bruin RA. Control of cell cycle transcription during G1 and S phases. *Nat Rev Mol Cell Biol*. 2013;14:518-528.
 46. Foster DA, Yellen P, Xu L, Saqcena M. Regulation of G1 cell cycle progression: distinguishing the restriction point from a nutrient-sensing cell growth checkpoint(s). *Genes Cancer*. 2010;1:1124-1131.
 47. Shi S, Tan P, Yan B, et al. ER stress and autophagy are involved in the apoptosis induced by cisplatin in human lung cancer cells. *Oncol Rep*. 2016;35:2606-2614.